Functional Materials 18, No.2 (2011)

Structure formation processes induced by the ion sputtering in anisotropic system with additive noise

V.O.Kharchenko

Institute of Applied Physics, National Academy of Sciences of Ukraine,
58 Petropavlovskaya St., 40030 Sumy, Ukraine

Received October 26, 2010

The processes of structure formation in an anisotripic system described by Kuramoto-Sivashinsky equation with additive noise as a generalization of the Bradley-Harper model for formation of surface structures induced by ion sputtering processes are studied. The time stability of the periodic spatial structures in the linean regime is considered. For a nonlinear model, the formation of various surface structures are studied, the power law of the surface growth is established, the roughness index and correlation fractal dimensionality of the respective structures are determined.

Исследованы процессы формирования структур в анизотропной системе, описываемой уравнением Курамото-Сивашинского с аддитивным шумом как обобщение модели Бредли-Харпера для формирования поверхностных структур, индуцируемых процессами ионного распыления. Рассмотрена временная устойчивость периодических пространственных структур для линейной модели. Для нелинейной модели изучены процессы формирования разных поверхностных структур, установлен степенной закон роста поверхности, определен показатель шероховатости и корреляционная фрактальная размерность соответствующих структур.

1. Introduction

Nanostructuring of solids has received much attention due to its potential application in electronics [1]. Among theoretical investigations, there are a lot of experimental data manifesting a large class of patterns appeared as a result of self-organization process on the surface of a solid. Ion beam sputtering is frequently regarded as a process for the fabrication of various nanostructured surfaces or interfaces. In the past few years, the ion-sputter erosion technique has aroused new interest as a method of producing nanodot/nanohole arrays on solid surfaces (see e.g. [2–9]). When a high energy ion enters a surface, several effects occur, including implantation, damage, mixing, electron emission, and chemical reactions, in addition to sputtering. It was shown experimentally that the main properties of pattern formation and structure of patterns (for example the size of nanodots/nanoholes or rows) depend on the energetic ion beam parameters such as ion flux, energy of deposition, ion dose, angle of incidence and temperature. Rows formation was studied on different substrates, i.e. on metals (Ag and Cu) [10, 11] on semiconductors (Ge [12] and Si [13–15]) on Sn [16], InP [17], on $Cd_2Nb_2O_7$ pyrochlore [18] and other. As was shown the height modulations on the surface induced by ion-beam sputtering result in rows formation having the typical size of 0.1 to 1 μm and nanoscale patterns with the linear size of 3.5 to 25 nm [19].

It is well known that the incidence angle has an influence on orientation of rows. Really, the wave vector of the modulations is parallel to the component of the ion beam in the surface plane at the incidence angles

around $\pi/2$, but perpendicular to that component at small incidence angles (close to grazing). In addition, the orientation of rows can be controlled by a penetration depth which is proportional to the deposition energy. A possibility of pattern formation control by both the incidence angle and penetration depth was shown in [4, 5]. The main theoretical models describing rows formation are based on results of the known works [3, 20–22].The main mechanisms for pattern formation were set to predict the orientation change of the roughness, formation of holes and dots. These models were generalized by taking into account additive fluctuations leading to statistical description of the corresponding processes.

In this article we aim to study the row (or generally pattern) formation processes in anisotropic system governed by the corresponding Kuramoto-Sivashinsky equation which takes into account additive noise caused by fluctuations of the beam flux. We consider the linear and nonlinear models separately and discuss the corresponding phase diagrams in the space of main beam parameters reduced to the penetration depths in each direction and the incidence angle. Moreover, we present results of the scaling behavior study of the correlation functions and discuss time dependences of the roughness and growth exponents during the system evolution as well as fractal properties of the surface. It will be shown that in the system under consideration, seven types of structures which can be formed with varying in incidence angle and penetration depths in each direction have fractal properties. We shall discuss phase diagrams and the scaling exponents in detail.

The work is organized in the following manner. In Section 2, we present the model for surface structures formation processes with additive noise. In Section 3, we discuss the stability analysis of the linear system. The nonlinear stochastic model is studied in Section 4. Here, we show the phase diagrams of patterning and consider the scaling properties of the correlation functions. The main results and prospects for the future are presented in the Conclusions.

2. Model

Let us consider a d-dimensional substrate and denote with $\mathbf{r}$ the d-dimensional vector locating a point on it. The surface is described at each time t by the height $z = h(\mathbf{r},t)$. If we assume the surface morphology is changed under ion sputtering, then we can use the model for the surface growth proposed in [3] and further developed in [4]. We consider the system where the direction of the ion beam lies in $x-z$ plane at an angle $\theta \in [0,\pi/2]$ to the normal of the uneroded surface. Following the standard approach, the average energy deposited at the surface (let say point O) due to the ion arriving at the point P in the solid is assumed to follow the Gaussian distribution [3];

$$E(\mathbf{r}) = \varepsilon/\left((2\pi)^{3/2}\sigma\mu^2\right)\exp(-z^2/2\sigma^2 - (x^2+y^2)/2\mu^2);$$

ε denotes the kinetic energy of the arriving ion, σ and μ are the widths of the distribution in directions parallel and perpendicular to the incoming beam. The parameters σ and μ depend on the target material and can vary with physical properties of the target and incident energy. The erosion speed at the surface point O is described by the formula $\nu = p\int\limits_R d\mathbf{r}\Phi(\mathbf{r})E(\mathbf{r})$, where integration is provided over the range of the energy distribution of all ions. Here $\Phi(\mathbf{r})$ is a correction for the local slope dependence of the uniform flux J which for surfaces with nonzero local curvature is defined by the general expression [23]:

$$\Phi(x,y,h) = J\cos(\arctan[\sqrt{(\nabla_x h)^2 + (\nabla_y h)^2}]).$$

The material constant p is defined by relation $p = 3/(4\pi^2)(NU_0C_0)^{-1}$, where U_0 and C_0 are the surface binding energy constants proportional to the square of the effective radius of the atomic interaction potential [23–25]. Hence, the dynamics of the surface height is defined by the relation $\partial_t h \approx -\nu(\theta - \nabla_x h, \nabla_x^2 h, \nabla_y^2 h)$ and is given by the equation $\partial_t h \approx -\nu(\theta)\sqrt{1+(\nabla h)^2}$ [3–5, 20, 26]. The linear term expansion gives $\partial_t h = -\nu_0 + \gamma\nabla_x h + \nu_x\nabla_{xx}^2 h + \nu_y\nabla_{yy}^2 h$. Here ν_0 is the surface erosion speed; $\gamma = \gamma(\theta)$ is a constant that describes the slope-depending erosion; $\nu_{x,y} = \nu_{x,y}(\theta)$ is effective surface tension generated by erosion process in each direction.

If the surface current is assumed to be driven by differences in chemical potential μ, then the evolution equation for the field h should take into account the term $-\nabla\cdot\mathbf{j}$ in the right-hand side, where $\mathbf{j_s} = K\nabla(\nabla^2 h)$ is

the surface current; $K > 0$ is the temperature-dependent surface diffusion constant. If the surface diffusion is thermally activated, then we have $K = D_s \kappa \rho / n^2 T$, where $D_s = D_0 e^{-E_a/T}$ is the surface self-diffusivity, E_a is the activation energy for surface diffusion, κ the surface free energy, ρ is the area density of diffusing atoms, n is the number of atoms per unit volume in the amorphous solid.

Assuming that the surface varies smoothly, we neglect spatial derivatives of the height h of third and higher orders in the slope expansion. Taking into account nonlinear terms in the slope expansion of the surface height dynamics, we arrive at the anisotropic Kuramoto-Sivashinsky equation for the quantity $h' = h + \nu_0 t$ of the form [3, 4]

$$\frac{\partial h}{\partial t} = \gamma \frac{\partial h}{\partial x} + \nu_x \frac{\partial^2 h}{\partial x^2} + \nu_y \frac{\partial^2 h}{\partial y^2} + \frac{\lambda_x}{2}\left(\frac{\partial h}{\partial x}\right)^2 + \frac{\lambda_y}{2}\left(\frac{\partial h}{\partial y}\right)^2 - K\nabla^4 h + \xi(x,y,t), \quad (1)$$

where we drop the primes for convenience and include additive noise with properties:

$$\langle \xi(\mathbf{r},t)\rangle = 0, \qquad \langle \xi(\mathbf{r},t)\rangle\langle \xi(\mathbf{r}',t')\rangle = 2\sum \delta(\mathbf{r}-\mathbf{r}')\delta(t-t'), \quad (2)$$

where $\sum$ is the noise intensity. Coefficients in Eq.(1) are defined in [4] and read

$$\gamma = F_0 \frac{s}{f^2} a_\sigma^2 a_\mu^2 c^2 (a_\sigma^2 - 1) - a_\sigma^4 s^2, \quad (3)$$

$$\nu_x = F_0 \frac{a_\sigma^2}{2f^3}\{2a_\sigma^4 s^4 - a_\sigma^4 a_\mu^2 s^2 c^2 + a_\sigma^2 a_\mu^2 s^2 c^2 - a_\mu^4 c^4\}, \quad (4)$$

$$\nu_y = -F_0 \frac{c^2 a\sigma^2}{2f}, \quad (5)$$

$$\lambda_x = F_0 \frac{c}{2f^4}\{a_\sigma^8 a_\mu^2 s^4 (3 + 2c^2) + 4a_\sigma^6 a_\mu^4 c^4 s^2 - a_\sigma^4 a_\mu^6 c^4 (1 + 2s^2) - f^2(2a_\sigma^4 s^2 - a_\sigma^2 a_\mu^2 (1 + 2s^2)) - a_\sigma^8 a_\mu^4 c^2 s^2 - f^4\}, \quad (6)$$

$$\lambda_y = F_0 \frac{c}{2f^2}(a_\sigma^4 s^2 + a_\sigma^2 a_\mu^2 c^2 - a_\sigma^4 a_\mu^2 c^2 - f^2). \quad (7)$$

In the above expressions we have defined

$$F_0 \equiv \frac{J\varepsilon p a}{\sigma\mu\sqrt{2\pi f}} \exp\left(\frac{-a_\sigma^2 a_\mu^2 c^2}{2f}\right), \quad (8)$$

$$a_\sigma \equiv \frac{a}{\sigma}, \quad a_\mu \equiv \frac{a}{\mu}, \quad s \equiv \sin(\theta), \quad c \equiv \cos(\theta), \quad f \equiv a_\sigma^2 s^2 + a_\mu^2 c^2. \quad (9)$$

Here all control parameters are defined by the ion penetration depths a_σ and a_μ, the incidence angle θ, the flux J and the kinetic energy ε. Next, we suppose $F_0 = 1$, $K = 2$ and $\sum = 1$.

3. Stability analysis of the linear model

It is known that transitions between two macroscopic phases in a given system occur due to the loss of the state stability at certain values of the control parameters. In the case of stochastic systems, the linear stability analysis needs to be done for a statistical moment of the perturbed state. We will now perform the stability analysis for the system with additive fluctuations. To that end, we average the Langevin equation (1) over the noise and get

$$\frac{\partial}{\partial t}\langle h\rangle = \gamma \frac{\partial}{\partial x}\langle h\rangle + \nu_x \frac{\partial^2}{\partial x^2}\langle h\rangle + \nu_y \frac{\partial^2}{\partial y^2}\langle h\rangle + \frac{\lambda_x}{2}\left\langle\left(\frac{\partial h}{\partial x}\right)^2\right\rangle + \frac{\lambda_y}{2}\left\langle\left(\frac{\partial h}{\partial y}\right)^2\right\rangle - K\nabla^4\langle h\rangle, \quad (10)$$

where we take into account the noise properties (2). Now, we can rewrite the linearized evolution equation for the average $\langle h\rangle$ in the standard form:

$$\frac{\partial}{\partial t}\langle h\rangle = (\hat{\nu}_{ef} + \hat{K}_{ef})\langle h\rangle, \quad (11)$$

with notations

$$\hat{\nu}_{ef} = \gamma \frac{\partial}{\partial x} + \nu_x \frac{\partial^2}{\partial x^2} + \nu_y \frac{\partial^2}{\partial y^2}, \quad \hat{K}_{ef} = -K\nabla^4. \quad (12)$$

Substituting solution

$$\langle h\rangle = A\exp(i[k_x x + k_y y - \omega t] + rt)$$

into Eq.(11) we arrive at relations for the frequency ω and stability parameter r:

$$\omega = -\gamma(\theta)k_x, \qquad r = -\nu_x(\theta)k_x^2 - \nu_y(\theta)k_y^2 - K(k_x^2 + k_y^2)^2. \quad (13)$$

From Eq.(13) and Eq.(5) it follows that average height $\langle h \rangle$ will be stable if $\nu_x > 0$. In Fig. 1 we show stability diagram of linear model. Here curves *1* and *2* correspond to dependences $a_\sigma(\theta)$ with $a_\mu = 1.5$ and $a_\mu = 0.5$, respectively. Curves *1′* and *2′* denote relations $a_\mu(\theta)$ at $a_\sigma = 1.5$ and $a_\sigma = 0.5$, respectively. We plot angle axes θ in radians (bottom) and in degrees (top) for convenience. The domain of stable solutions denoted as $\nu_x > 0$ is on the right of curves. It is seen from Fig. 1 that increasing in a_μ restricts the stability domain (curves *1* and *2*), whereas increasing in a_σ (curves *1′* and *2′*) in contrast expands this domain. In the insertion we show snap-shots in time 20, 100 and 500 (from top to bottom) of typical structures in domains of stable and unstable solutions. It is seen that in the domain of stable solutions, there are well-defined periodical structures stable in time, whereas if $\nu_x < 0$, the structures have not periodicity and well-defined orientation. In our simulations, we have used Gaussian initial conditions by taking $\langle h(\mathbf{r}, t = 0) \rangle = 0$, $\langle (\delta h)^2 \rangle = 0.1$; integration time step is $\Delta t = 0.005$, space step is *ell* = 1.

4. Nonlinear stochastic model

Now let us consider the nonlinear system behavior setting $\lambda_x \neq$ and $\lambda_y \neq 0$. In the following study, we are based on the simulation procedure, solving nonlinear stochastic differential equation (1).

4.1. *Surface morphology changing*. We shall consider an anisotropic system where erosion constant $\gamma = 0$. We have computed phase diagrams for the nonlinear systems illustrating formation of different patterns shown in Fig. 2. Let us consider diagram $a_\sigma(\theta)$ at $a_\mu = 0.25$ shown in Fig. 2a. Here, the whole plane (a_μ, θ) is divided into 10 regions, denoted by A, B, C, D, E, F, G and characterized by sign of ν_x, λ_x, λ_y, ($\nu_x < 0$ for all regions due to Eq.(5)). In the Figure, dashed lines correspond to a change of the sign of λ_x, dot line defines condition $\nu_x = 0$, λ_y equals zero in the dash-dot line and if solid line is crossed then as λ_x as λ_y changes its sign. It is important that at $a_\sigma \leq a_\mu$, one has known phase diagram where ν_x, λ_x, change sign and only three different domains (A, B and C) are realized. At that time, if $a_\sigma > a_\mu$, then there are seven domains which correspond to different structures. In Fig. 2b we show dependences $a_\mu(\theta)$

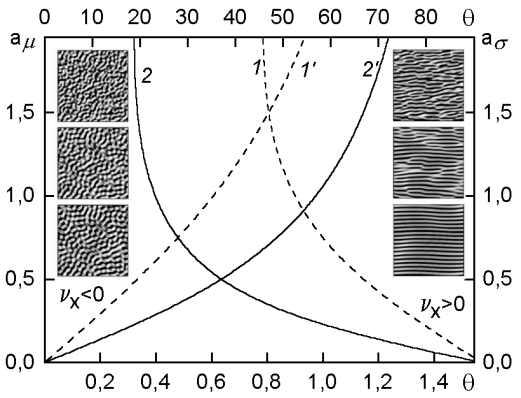

Fig. 1. Diagram of temporal stability for periodical structures of linear model (curves *1* and *2* correspond to dependences $a_\sigma(\theta)$ with $a_\mu = 1.5$ and $a_\mu = 0.5$, *1′* and *2′* denote dependences $a_\mu(\theta)$ with $a_\sigma = 1.5$ and $a_\sigma = 0.5$).

at $a_\sigma = 2.0$. Here lines are defined as in a previous graph. Figs. 2c and 2d illustrate dependences $a_\mu(a_\sigma)$ at small ($\theta = 0.2$) and large ($\theta = \pi/2 - 0.2$) angles, respectively. In Fig. 2c, the dash-dot-dot line corresponds to the condition $\nu_x = \lambda_x = 0$. Comparing Figs. 2c and 2d one can see that an increase in angle of incidence results in reduction of region G and invokes large values of a_μ for regions A and B. Typical structures in all possible regions are shown in Fig. 3.

Let us consider a morphology changing of patterns with respect to signs of ν_x, λ_x and λ_y. A linear stability analysis shows that the sign of ν_x determines the stability of solutions. In other words, $\nu_x < 0$ is a condition of instability in *x*-direction existence ($\nu_y < 0$ for always due to Eq.(5)). So, the main criterion of a nanodots/nanoholes formation is $\nu_x < 0$ (see regions A, B, F, G). Investigation of the noiseless anisotropic Kuramoto-Sivashinsky equation shows that when $\lambda_x \cdot \lambda_y < 0$ a direction of rows being rotated with respect to the ion direction (see regions B, C, E, F). The additional criterion of a nanodots/nanoholes formation is $\lambda_x \cdot \lambda_y > 0$. Thus, a fabrication of nanodots/nanoholes is provided by conditions $\nu_x < 0$ and $\lambda_x \cdot \lambda_y > 0$ (see regions G and A and corresponding structures in Fig. 3, respectively).

In contrast to the previous case, the main condition of rows formation in *x* direction is $\nu_x > 0$ and the additional one is $\lambda_x \cdot \lambda_y < 0$ (see regions C and E and corresponding structures in Fig. 3). For regions B, D, and F the following nanodots/nano-

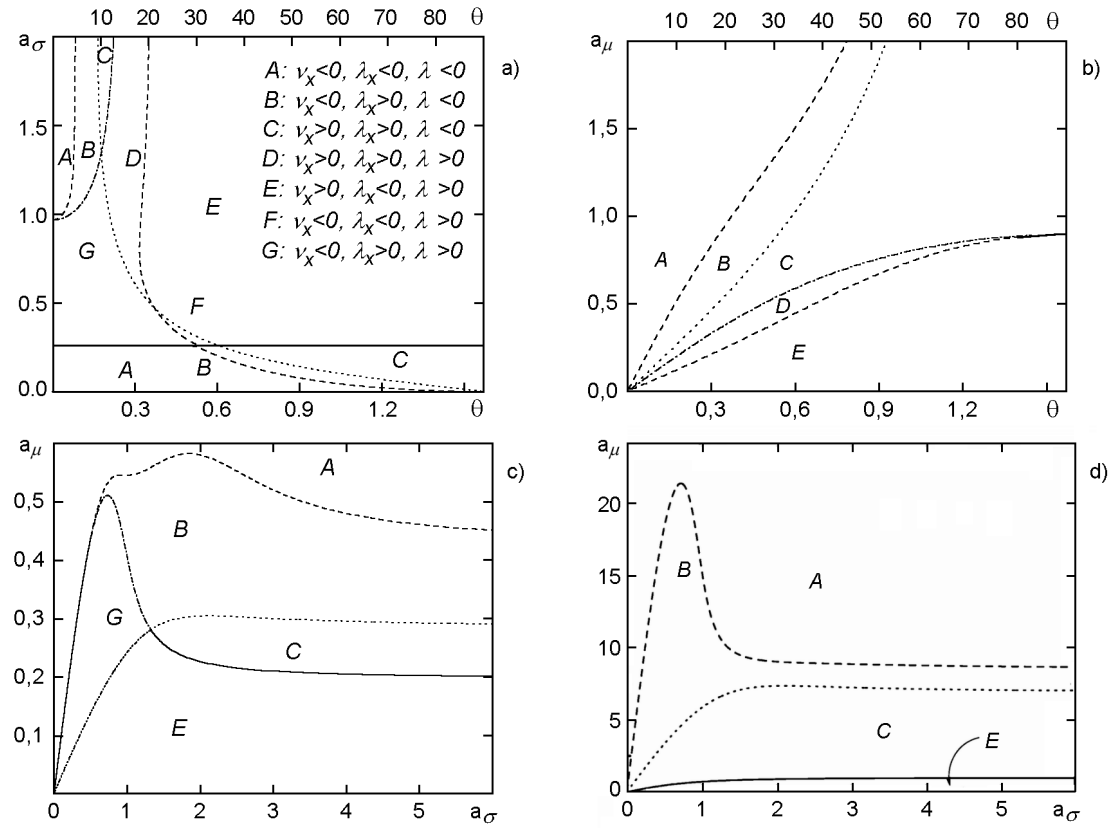

Fig. 2. Phase diagrams for the nonlinear systems illustrating formation of different patterns at: $a_\mu = 0.25$ (a), $a_\sigma = 2.0$ (b), $\theta = 0.2$ (c), $\theta = \pi/2 - 0.2$ (d).

holes formation criteria are valid, as row and ripples formation ones do not satisfy: structures B and F are characterized by negative values of ν_x (existence of instability in x- and y-directions) but different signs of λ_x and λ_y become to rotating of the row with respect to the ion direction; in region D with positive values of ν_x the product $\lambda_x \cdot \lambda_y > 0$ does not provide the formation of well defined structures on surface.

The shape of structures A and G, B and F, C and E is topologically identical: structures A, B and C are concave and structures E, F, G and D are convex. The type of a structure (convex or concave) is determined by the sign of λ_y. The system under consideration does not generate concave-like structures, identically to structures from D region.

To prove that structures A and G in Fig. 3 are stable in time, we compute the number of nanodots/nanoholes vs time. Corresponding dependences are shown in Fig. 4. It is seen that as for process of nanodots formation (see filled circles), as for process of nanoholes formation (see empty circles) the number $n = N/N_{max}$ of "islands" increases at small time ($t < 400$) that corresponds to processes of "islands" formation. At intermediate time ($400 < t < 600$), a relative number of "islands" falling down that relates to coalescence processes of "islands". At large time $t > 600$, one has stationary behavior of a relative number of "islands". So, it follows that processes of nanodots/nanoholes formation are stationary: when the growth and coalescence processes are finished the average number of "islands" does not change in time.

4.2. *Scaling properties of the surface morphology*. Using numerical data, it is possible to study the statistical properties of the system considering the time-dependent height-height correlation function, determined in the following manner: $C_h(\mathbf{r},t) = \langle (h(\mathbf{r}+\mathbf{r}',t) - h(\mathbf{r}',t))^2 \rangle$. In the framework of the dynamic scaling hypothesis, the correlation function can be written in the following form [27, 28]:

$$C_h = (\mathbf{r},t) = 2W^2(t)\varphi\left(\frac{r}{\zeta(t)}\right), \qquad (14)$$

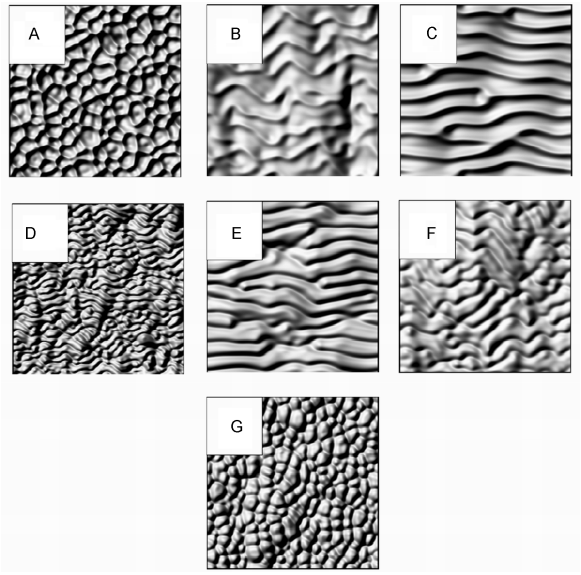

Fig. 3. Typical structures in regions A–G at t = 420, 1780, 1440, 40, 600, 700 and 320, respectively.

where $W^2 = \langle (h(\mathbf{r}) - \langle h(\mathbf{r}) \rangle)^2 \rangle$, W is the interface width, and

$$\varphi(u) \approx \begin{cases} u^{2\alpha}, & \text{for } u << 1, \\ \text{const}, & \text{for } u >> 1. \end{cases} \qquad (15)$$

Early stages can be fitted by the function $C_h(\mathbf{r},t) \approx 2W^2(t)[1 - \exp[-(r/\zeta)^{2\alpha}]$ [29]. The dynamic scaling hypothesis assumes that the following dependences are valid: $W^2(t) \propto t^{2\beta}$, $\zeta(t) \propto t^{1/z}$, where β is the growth exponent, z is the dynamic exponent for which $z = \alpha/\beta$. From another viewpoint, we can assume [30]

$$C_h(\mathbf{r},t) = r^{2\alpha}\psi\left(\frac{t}{r^2}\right), \qquad (16)$$

where

$$\psi(\nu) \approx \begin{cases} \nu^{2\beta}, & \text{for } \nu << 1, \\ \text{const}, & \text{for } \nu >> 1. \end{cases} \qquad (17)$$

Therefore, these two cases lead to the results $C_h(t) \propto t^{2\beta}$ and $C_h(r) \propto r^{2\alpha}$, allowing to define the growth exponent β and the roughness exponent α. As was shown in [30, 31], the roughness $W(t,L)$ can be related to the structure function $S(\mathbf{k})$ as follows

$$W^2(t,L) = V^{-1}\sum\nolimits_{k \neq 0} S(\mathbf{k},t),$$

where $S_h(k,t) = V^{-1}\langle h_k(t)h_{-k}(t)\rangle$. The structure function (k,t) has the form

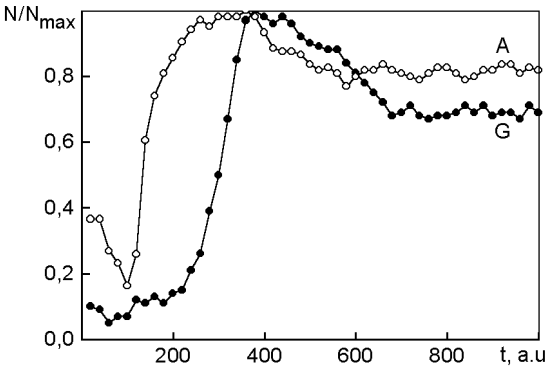

Fig. 4. Dependences of the relative number of nanodots and nanoholes vs time.

$$S_h(k,t) = k^{-(d+2\tilde{\alpha})}\Theta(k^2 t), \qquad (18)$$

with spatial dimension $d = 2$ where

$$\Theta(k^z t) \approx \begin{cases} k^{2\alpha}t^{2\alpha/\beta}, & \text{for } k^z t << 1, \\ \text{const}, & \text{for } k^z t >> 1, \end{cases} \qquad (19)$$

and scales as $S_h(k,t) \propto k^{-(d+2\tilde{\alpha})}$ for large t and $S_h(k,t) \propto t^{2\beta}$ for small .

In previous studies (see for example [6]), it was shown that even in the isotropic system with additive noise the scaling exponents α, β and z depend on the system parameters ν, λ and K. Moreover, these exponents are the time-dependent functions, i.e. its magnitudes can be changed in the course of the system evolution. According to the scaling hypothesis, the temporal evolution of the quantity $W = \langle (\delta h)^2 \rangle$, where $\delta h = h - \langle h \rangle$, can be represented through the exponent β.

To characterize fractal properties of the surface, we can study a pair correlation function defined as follows:

$$C_p(\mathbf{r};t) = \langle h(\mathbf{r} + \mathbf{r}',t)h(\mathbf{r},t) \rangle. \qquad (20)$$

If there is no characteristic space scale, then the introduced correlation function should behave itself algebraically, i.e., $C_p(r,t) \propto 1/r^{\Delta}$, where the scaling exponent Δ relates to the fractal correlation dimension D_2 as $\Delta = d - D_2$. The corresponding Fourier transformation of the correlation function $C_p(\mathbf{r},t)$ scales as $S_p(k,t) \propto k^{-D_2}$. From the definition of the correlation fractal dimension D_2 and the properties of the Fourier component of the correlator (20) it follows that at $D_2 = 0$ there is no scaling behavior of the structure function and $S_p(k,t) \approx const$. Hence, the surface at the

fixed time t can be considered as a Gaussian surface with no correlation, i.e. white noise in space with equal contribution of all wavenumbers k; the corresponding spatial correlator (20) is reduced to the Dirac delta-function, $C_p(\mathbf{r}) \to \delta(\mathbf{r})$. In the case $D_2 = 0$, one arrives at typical dependence $S_p(k) \propto k^{-2}$ for diffuse spreading on the well structured surface. Here the topological dimension d equals the fractal dimension D_2.

We have performed calculations of the scaling exponents for each structure in Fig. 3. We have computed sets $\{\alpha_i\}$ and $\{\beta_i\}$ at time window when the interface width W or the correlation function $C_h(r)$ start to grow until their saturation (i.e., when algebraic dependences $W^2(t) \propto t^{2\beta}$ and $C_h(r) \propto r^{2\alpha}$ are observed). We compute the corresponding pair correlation function $C_p(r;t)$ and the associated fractal dimension D_2 specially for each structure in Fig. 3. The corresponding sets $\{\alpha_i\}$ and $\{\beta_i\}$ for each structure are shown in Fig. 5. Fig. 5a illustrates set $\{\beta_i\}$ (the top panel represents dependences $\{\beta_i\}$ vs time for deterministic model with $\sum = 0$, the bottom panel shows the same dependences for stochastic model at $\sum = 1.0$); in Fig. 5b, we plot the roughness exponents $\{\alpha_i\}$ (error bars represent the standard deviation of the mean results).

It is seen from Fig. 5a that exponents β_i, which define the growth law of corresponding structures in time have different values. The time dependence means that at early stages where growth processes are realized there is a straight line for $W^2(t)$ in log-log plot. At large time limit where coarsening processes start to play essential role, there is a set of exponents $\{\beta_i\}$. Such set means that the local power-law approximation can be used for the smooth function $W^2(t)$ where each exponent β_i relates to the fixed time interval Δt_i: $W^2(\Delta t_i) \propto (\Delta t_i)^{2\beta_i}$. According to such assumption, the function $\varphi(\cdot)$ in Eq.(15) should behave itself in a more complicated form on a given time interval Δt_i than the simplest power law shown above. The proposed approximation allows to study at what time interval nonlinear effects are responsible for the system evolution. It can be seen that as for deterministic model (top panel) as for stochastic one (bottom panel) initially β_i start to increase until a maximum is reached; then β_i decreases. It takes maximal value more later for structures B and C (time $t \approx 600$ and $t \approx 800$) than for structures A, E, F, G and D ($t \approx 150 \div 300$ and $t \approx 20$). Comparing results of $\{\beta_i\}$ for deterministic and stochastic models we can conclude that during the system evolution, β_i grows faster for deterministic system than it is for stochastic one. It means that the coarsening processes in deterministic case occur faster than in the stochastic one. From physical viewpoint, it means that additive noise promotes slowdown of growth processes: they are delayed in time (in a short time interval with small $\beta_i < 1$). Moreover, coarsening processes are accelerated without of noise: they occur with $1 < \beta_i < 7$. In stochastic system, the growth processes occur later than at $\sum = 0$, whilst coarsening ones are decelerated with $1 < \beta_i < 3.5$. Therefore, the additive noise

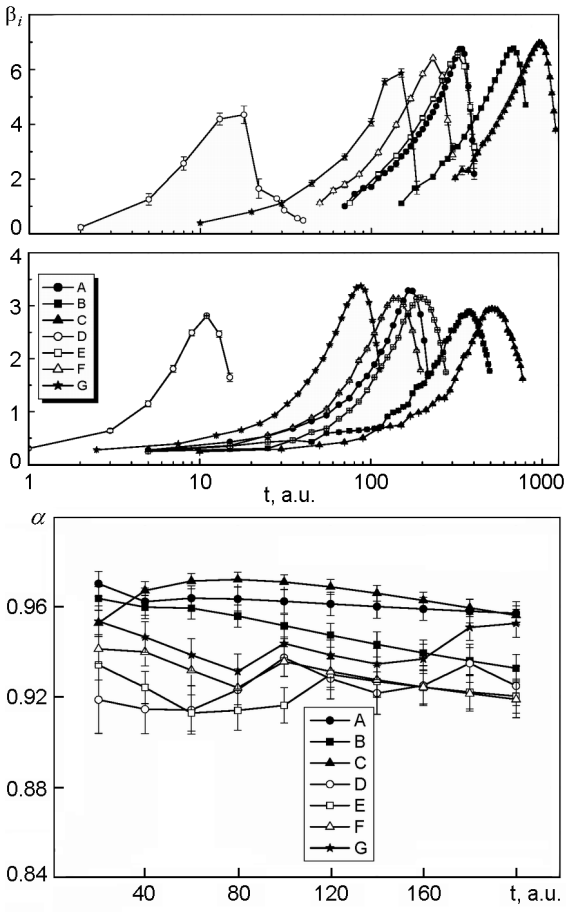

Fig. 5. Scaling exponents for the structures in Fig. 3: a) the set of the growth exponent β_i (top panel represents results for deterministic system with $\sum = 0$; bottom one shows results for stochastic system with $\sum = 1.0$), b) the roughness exponent α.

in anisotropic systems is able to delay growth and coarsening processes (it halves values of the growth exponent at large time interval) from one hand. From another one, it is responsible for decreasing the time interval where these processes are realized.

From Fig. 5b, it can be concluded that the roughness exponents $\{\alpha_i\}$ do not change its values in time for each structure from Fig. 3. Small deviations from a mean value are within the bounds of error.

It is known that at large time intervals, the exponents $\tilde{\alpha}$ can be determined from the definition $S_h(k) \propto k^{-(d+2\tilde{\alpha})}$, where $d = 2$. We have computed the spherically averaged structure function defined on a circle

$$S_h(k,t) = 1/N_k \sum_{k \le \mathbf{k} \le k+\Delta k} S_h(\mathbf{k}, t)$$

where N_k is the number of points on the circle of the width Δk. Comparison of results for the exponents α_i and $\tilde{\alpha}$ obtained from relations $C_h(r) \propto r^{2\alpha}$ and $S_h(k) \propto k^{-(d+2\tilde{\alpha})}$, respectively, for all structures shows a difference in $0.5 \div 1.5$ %.

We have computed the fractal dimension D_2 for all structures in Fig. 3. We have found that the fractal properties are well pronounced for the structure A characterizing by the fractal dimension $D_2^{(A)} \approx 1.891$, whereas structures B and G are well structural patterns with $D_2^{(B)} \approx 1.996$ and $D_2^{(C)} \approx 1.995$. Structures C, D, E and F are characterized by light fractal properties with $D_2 = 1.952 \div 1.989$.

5. Conclusions

We have studied the patterns formation processes induced by the ion sputtering under stochastic conditions of illumination in anisotropic system. The main assumption was the stochastic nature of the beam flux. We have discussed phase diagrams of different patterns in both linear and nonlinear models. Within the framework of the linear stability analysis, we have found critical values of incidence angle at fixed values of penetration depths which define surface structures.

Studying the nonlinear model, we have computed the phase diagrams illustrating formation of different patterns (ripples, holes and dots) which relates to the results from the linear stability analysis. The main properties of the pattern formation processes were studied with the help of interface width and correlation functions. We have shown that patterns, characterizing by nano-holes and nano-dots are stable in time (a number of holes/dots is a constant at large time). To make a detailed analysis of the pattern formation, we have examined the scaling behavior of main statistical characteristics of the system reduced to the correlation functions and its Fourier transforms (structure functions). We have computed the scaling exponent for all possible realizing structures. It was shown that the additive noise in anisotropic systems is able to delay the growth and coarsening processes and decreases the time interval where these processes are realized. We have calculated the fractal (correlation) dimension. It was shown that all patterns have fractal properties.

References

1. L.Jacak, P.Hawrylak, A.Wojs, Quantum Dots, Springer-Verlag, Berlin (1998).
2. M.Navez, C.Sella, D.Chaperot, Ionic Bombardment: Theory and Applications, ed. by J.J.Trillat, Gordon and Breach, New York (1964).
3. R.M.Bradley, J.M.E.Harper, *J. Vac. Sci. Technol. A*, **6**, 2390 (1988).
4. R.Cuerno, A.-L.Barabasi, *Phys. Rev. Lett.*, **74**, 4746 (1995).
5. M.Makeev, A.-L.Barabasi, *Appl. Phys. Lett.*, **71**, 2800 (1997).
6. J.T.Drotar, Y.-P.Zhao, T.-M.Lu, G.-C.Wang, *Phys. Rev. E*, **59**, 177 (1999).
7. T.Aste, U.Valbusa, *Physica A*, **332**, 548 (2004).
8. B.Kahng, J.Kim, *Curr. Appl. Phys.*, **4**, 115 (2004).
9. R.Kree, T.Yasseri, A.K.Hartmann, *Nucl. Instr. Meth. Phys. Res. B*, **267**, 1407 (2009).
10. S.Rusponi, C.Boragno, U.Valbusa, *Phys. Rev. Lett.*, **78**, 2795 (1997).
11. S.Rusponi, G.Costantini, C.Boragno, U.Valbusa, *Phys. Rev. Lett.*, **81**, 2735 (1998).
12. E.Chason, T.M.Mayer, B.K.Kellerman et al., *Phys. Rev. Lett.*, **72**, 2040 (1994).
13. J.Erlebacher, M.J.Aziz, E.Chason et al., *Phys. Rev. Lett.*, **82**, 2330 (1999).
14. W.-Q.Li, L.J.Qi, X.Yang et al., *Appl. Surf. Sci.*, **252**, 7794 (2006).
15. W.J.MoberlyChan, D.P.Adams, M.J.Aziz et al., *MRS Bulletin*, **32**, 424 (2007).
16. H.X.Qian, W.Zhou, Y.Q.Fu et al., *Appl. Surf. Sci.*, **240**, 140 (2005).
17. D.Paramanik, S.Majumdar, S.R.Sahoo et al., *J. Nanosci. and Nanotech*, **8**, 1 (2008).
18. J.Lian, Q.M.Wei, L.M.Wang et al., *Appl. Phys. Lett.*, **88**, 093112 (2006).
19 S.Facsko, T.Dekorsy, C.Koerdt et al., *Science*, **285**, 1551 (1999).

20. M.Kardar, G.Parisi, Y.-C.Zhang, *Phys. Rev. Lett.*, **56**, 889 (1986).
21. D.E.Wolf, J.Villian, *Europhys. Lett.*, **13(5)**, 389 (1990).
22. Y.Kuramoto, T.Tsuzuki, *Prog. Theor. Phys.*, **55**, 356 (1977).
23. M.A.Makeev, A.-L.Barabasi, *Nucl. Instr. Meth. Phys. Res. B*, **222**, 316 (2004).
24. P.Sigmund, *J. Matter. Sci*, **8**, 1545 (1973).
25. P.Sigmund, *Phys. Rev.*, **184**, 383 (1969).
26. J.W.Cahn, J.E.Taylor, *Acta Metall. Matter*, **42**, 1045 (1994).
27. F.Family, T.Vicsek, *J. Phys. A*, **18**, L75, (1985).
28. F.Family, *Physica A*, **168**, 561 (1990).
29. S.K.Sinha, E.B.Sirota, S.Garott, *Phys. Rev. B*, **38**, 2297 (1988).
30. L.Giada, A.Giacometti, M.Rossi, *Phys. Rev. E*, **65**, 036134 (2002).
31 D.O.Kharchenko, V.O.Kharchenko, I.O.Lysenko, S.V.Kokhan, *Phys. Rev. E*, 82, 061108, (2010).

Процеси формування структур при іонному розпиленні в анізотропній системі з адитивним шумом

В.О.Харченко

Досліджено процеси формування структур у анізотропній системі, що описується рівнянням Курамото-Сівашинського з адитивним шумом, як узагальнення моделі Бредлі-Харпера для формування поверхневих структур, що індуковані процесами іонного розпилення. Проведено аналіз часової стійкості періодичних просторових структур для лінійної моделі. Для нелінійної моделі вивчено процеси формування різних поверхневих структур, встановлено степеневий закон росту поверхні, визначено показник шорсткості та кореляційну фрактальну розмірність відповідних структур.